

1 DNA methylation facilitates local adaptation and adaptive transgenerational 2 plasticity

3
4 Melanie J. Heckwolf^{1*}, Britta S. Meyer^{1,##}, Robert Häsler², Marc P. Höppner², Christophe
5 Eizaguirre³ and Thorsten B. H. Reusch¹

6
7 * *equal contribution*

8 ¹ *Marine Evolutionary Ecology, GEOMAR Helmholtz Centre for Ocean Research Kiel, Kiel,*
9 *Germany*

10 [#] *present address: Max Planck Research Group Behavioural Genomics, Max Planck Institute for*
11 *Evolutionary Biology, Plön, Germany*

12 ² *Institute of Clinical Molecular Biology, Kiel University, Kiel, Germany*

13 ³ *School of Biological and Chemical Sciences, Queen Mary University of London, London, UK*

15 **Keywords**

16 DNA methylation, epigenetics, *Gasterosteus aculeatus*, local adaptation, phenotypic plasticity,
17 reduced representation bisulfite sequencing, transgenerational acclimation

19 **Abstract**

20 Epigenetic inheritance has been suggested to contribute to adaptation via two distinct pathways.
21 Either, stable epigenetic marks emerge as epimutations and are targets of natural selection via
22 the phenotype, analogous to adaptation from DNA sequence-based variation. Alternatively,
23 epigenetic marks are inducible by environmental cues, possibly representing one mechanism of
24 transgenerational phenotypic plasticity. We investigated whether both postulated pathways are
25 detectable in nature and sequenced methylomes and genomes of three-spined sticklebacks

26 (*Gasterosteus aculeatus*) across a natural salinity gradient in a space-for-time approach.
27 Consistent with local adaptation patterns, stickleback populations showed differentially
28 methylated CpG sites (pop-DMS) at genes enriched for osmoregulatory processes. In a two-
29 generation salinity acclimation experiment with fish from the mid salinity, we found the majority
30 (62%) of pop-DMS to be insensitive to experimental salinity change, suggesting that they were
31 shaped by selection and facilitate local salinity adaptation. Among the experimentally inducible
32 DMS, two-thirds increased in similarity to anticipated adaptive patterns in wild populations under
33 exposure to the novel salinity. This study demonstrates the presence of two types of methylation
34 marks, inducible and stable, that contribute to adaptive transgenerational plasticity and local
35 adaptation in natural populations.

36

37 **Main text**

38 Recent advances in epigenetics have started to challenge our understanding of inheritance and
39 adaptive evolution^{1, 2, 3}. It has been suggested that epigenetic inheritance provides an additional
40 evolutionary pathway to adaptive phenotypes^{4, 5}, involving the heredity of molecular variation
41 such as DNA methylation, histone modification and small RNAs⁶. Several theoretical models
42 posit that heritable variation of these molecular modifications can contribute to adaptation to
43 environmental change via two distinct information pathways^{5, 7, 8}. Firstly, *selection-based*
44 epigenetic marks can emerge as spontaneous epimutations that remain stable across
45 generations, regardless of the current environment⁷. These epimutations underlie phenotypes
46 that are targets of natural selection similar to adaptation from DNA sequence-based variation^{5, 8,}
47 ⁹. Secondly, *detection-based* effects describe inducible epigenetic marks under environmental
48 control and are hypothesized to be a transgenerational form of phenotypic plasticity^{7, 10}. While
49 the significance and principal difference of both transmission pathways have been
50 acknowledged^{4, 5, 7}, empirical evidence for the quantification of adaptive epigenetic variation
51 along with its transgenerational inducibility is rare, especially in natural populations (but see

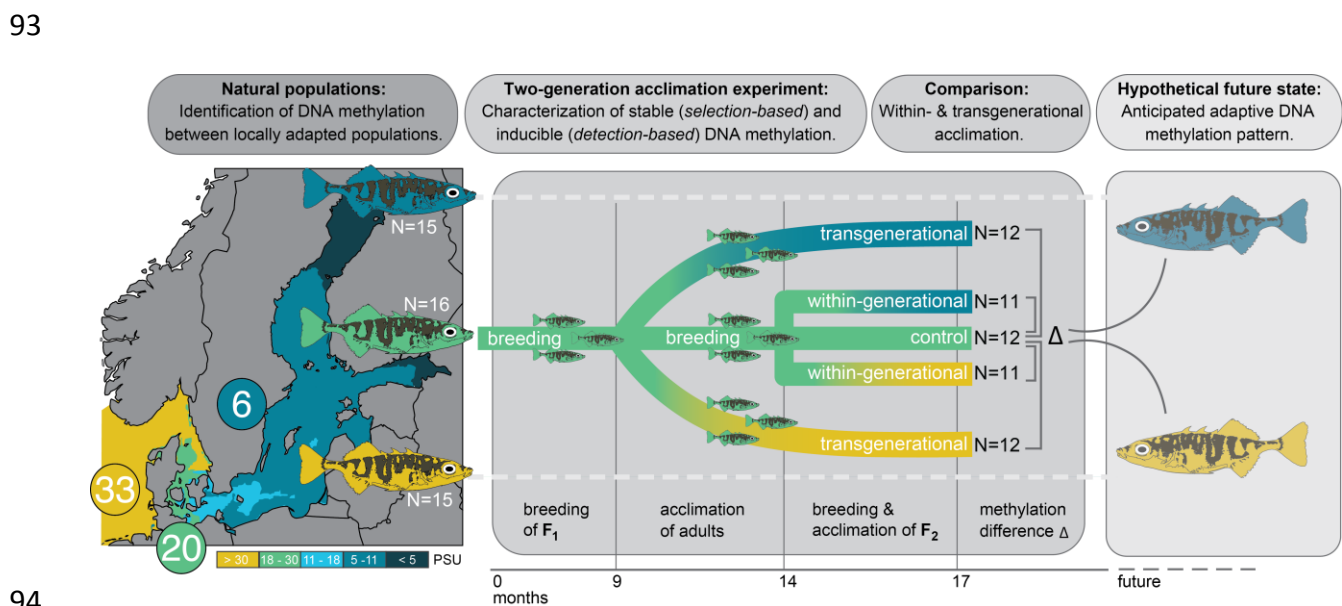
52 references^{10, 11, 12}). One prime objective of this study was thus to assess whether these two
53 epigenetic pathways can be detected in nature and to test whether short term acclimation
54 responses match patterns of DNA methylation variation of natural populations. If
55 transgenerational experiments result in DNA methylation profiles closer to those of locally
56 adapted natural populations, this would provide evidence that DNA methylation is
57 mechanistically involved in adaptive transgenerational plasticity.

58 Studying the adaptation to ocean salinity is particularly well suited to identify *selection-*
59 *based* and *detection-based* effects, as changes in salinity are predicted to be gradual over time
60 and experiments can easily be carried out with average values, as ocean salinity varies less
61 depending on the season than temperature for instance. Since salinity change imposes strong
62 physiological stress with well-defined cellular effects¹³, natural salinity gradients offer unparalleled
63 opportunities to use local patterns of epigenetic variation as background against which direction
64 and magnitude of experimental salinity manipulations can be tested. One suitable ecosystem to
65 follow such a space-for-time approach is the Baltic Sea, a semi-enclosed marginal sea that has
66 been dubbed a time machine for many predicted perturbations associated with global change¹⁴.

67 Taking advantage of this natural large-scale salinity gradient, we sequenced the
68 methylomes (reduced representation bisulfite sequencing, RRBS) as well as whole genomes of
69 three-spined sticklebacks (*Gasterosteus aculeatus*) from three locally adapted populations¹⁵ in-
70 and outside the Baltic Sea salinity gradient (6, 20 and 33 PSU). Baltic stickleback populations
71 are genetically differentiated from one another (genome wide average pairwise $F_{ST} = 0.028$ ¹⁵)
72 and show patterns consistent with local adaptation to salinity regimes in controlled common
73 garden experiments^{16, 17}. Furthermore, sticklebacks are known for their adaptive
74 transgenerational plasticity in response to variation in temperature¹⁸ and changes in DNA
75 methylation levels at osmoregulatory genes in response to within generation salinity
76 acclimation^{19, 20}. However, it remains unclear whether DNA methylation facilitates adaptive
77 transgenerational plasticity, a mechanism hypothesized to facilitate phenotypic adaptation to

78 rapid environmental change. To address this question, we complemented our field survey with a
 79 two-generation salinity acclimation experiment using the mid salinity population (20 PSU) to
 80 quantify the proportion of stable (potentially *selection-based*) and inducible (potentially *detection-*
 81 *based*) DNA methylation within- and across generations (Figure 1). We focused on the
 82 methylation of cytosines at cytosine-phosphate-guanine dinucleotides (CpG sites), the most
 83 common methylation motif in vertebrates²¹ with partial inheritance potentially facilitating
 84 adaptation in natural populations¹⁰.

85 We tested three hypotheses: (i) Stickleback populations originating from different salinity
 86 areas (6, 20 and 33 PSU) show differentially methylated CpG sites (pop-DMS), consistent with
 87 patterns of local adaptation. (ii) Such pop-DMS include experimentally stable, in the form of
 88 population-specific, and experimentally inducible, in the form of environment-specific,
 89 methylation sites. (iii) Upon transgenerational salinity acclimation, inducible DNA methylations
 90 become more similar to the patterns of natural populations at corresponding salinities. Along
 91 with the functional enrichment assessment, the latter findings would be evidence of a
 92 mechanism of adaptive transgenerational plasticity.



95 **Figure 1: Experimental space-for-time approach.** We characterized DNA methylation profiles (via
 96 Reduced Representation Bisulfite Sequencing, RRBS) and whole genomes (Whole Genome Sequencing,

97 WGS) of fish from three populations of wild caught three-spined sticklebacks locally adapted to 6 (blue, N
98 = 15), 20 (green, N = 16) and 33 PSU (yellow, N = 15). We also collected sticklebacks from the mid
99 salinity location (20 PSU) and acclimated laboratory bred offspring of these fish within one ('within-
100 generational') or over two ('transgenerational') generations to decreased (6 PSU) or increased (33 PSU)
101 salinity, and maintained a control group at its original salinity (N = 11-12 per group, see details in Figure).
102 Differential methylation within and across generations was assessed and compared to natural populations
103 locally adapted to the corresponding salinity, serving as the hypothetical future DNA methylation state to
104 capture long term adaptation processes.

105

106 **Identifying differentially methylated CpG sites across wild populations along a salinity**

107 **cline**

108 In order to identify differentially methylated CpG sites (DMS) between stickleback populations
109 along the salinity cline in- and outside of the Baltic Sea (hereafter pop-DMS), we sequenced the
110 methylome (RRBS) of 46 wild caught sticklebacks from 3 different salinity regimes (Sylt, 33
111 PSU; Kiel, 20 PSU; Nynäshamn, 6 PSU; Figure 1). After quality and coverage filtering, we
112 obtained 525,985 CpG sites present in all groups, corresponding to ~4% of all CpG sites in the
113 stickleback genome. Between pairs of wild caught populations, we detected 1,470 (comparison
114 20 vs. 6 PSU) and 1,158 (20 vs. 33 PSU) pop-DMS. The distribution of these sites was random
115 with regard to the genomic features (promoter, exon, intron, and intergenic; 20 vs. 6 PSU: $\chi^2_3 =$
116 3.36, $P = 0.340$; 20 vs. 33 PSU: $\chi^2_3 = 1.61$, $P = 0.656$; Supplementary Material: Figure S1 and
117 Table S1) and regions along the chromosomes (Supplementary Figure S3A). Noteworthy,
118 among these pop-DMS, 1,098 (20 vs. 6 PSU) and 871 (20 vs. 33 PSU) were located close to (<
119 10 kb from transcription start sites) or within genes thereby associated with 655 and 510 genes,
120 respectively. Many of these genes were involved in basic biological processes such as ectoderm
121 development, DNA-repair and strand renaturation, as well as chromatid segregation and
122 chromosome condensation (Figure 2). Particularly relevant and concordant with previous

123 findings of local salinity adaptation¹⁵, these genes were enriched for osmoregulatory processes
124 such as ion transport and channel activity, renal water homeostasis and absorption. Genes
125 associated with ≥ 10 pop-DMS are listed in Table 1 (for all genes, see Supplementary Table S2A
126 and S2B). Since local adaptation is 10-fold more likely to involve changes at the gene
127 expression than at the amino acid sequence level^{22, 23}, it is conceivable that differential DNA
128 methylation and consequently different regulation of osmoregulatory genes facilitates local
129 adaptation to salinity. Remarkably, one of the top candidate genes differentially methylated
130 between populations from 20 and 6 PSU was *eda* (*Ectodysplasin A*), a well-described gene
131 involved in lateral plate formation²⁴. Salinity and calcium are significant drivers of plate
132 morphology²⁵ in proposed conjunction with predation²⁶. Our findings suggest that repeated and
133 parallel selection for the low plated *eda* allele in response to low saline habitats^{27, 28, 29}, including
134 the Baltic Sea^{15, 30}, may involve methylation mechanisms. Taken all together, our results suggest
135 that, along with genetic differentiation, differentially methylated genes likely contribute to local
136 salinity adaptation across stickleback populations (Figure 2, Table 1; Supplementary Material:
137 Figure S2, Table S2A and S2B). To further investigate this hypothesis, we experimentally
138 characterized the proportion of stable (population-specific) and inducible (environment-specific)
139 pop-DMS.

140

141 **Characterizing stable and inducible DNA methylation in a two-generation experiment**

142 In order to distinguish between stable and inducible DNA methylation we then conducted a two-
143 generation salinity acclimation experiment with laboratory bred sticklebacks from the mid salinity
144 population (Figure 1). We considered pop-DMS to be stable when both the within- and the
145 transgenerational acclimation group were not differentially methylated compared to the control
146 group (q -value ≥ 0.0125). These population-specific and environmentally insensitive pop-DMS
147 could be a target for natural selection via the phenotype (*sensu selection-based*⁷). On the other
148 hand, if a pop-DMS was also differentially methylated between at least one of the acclimation

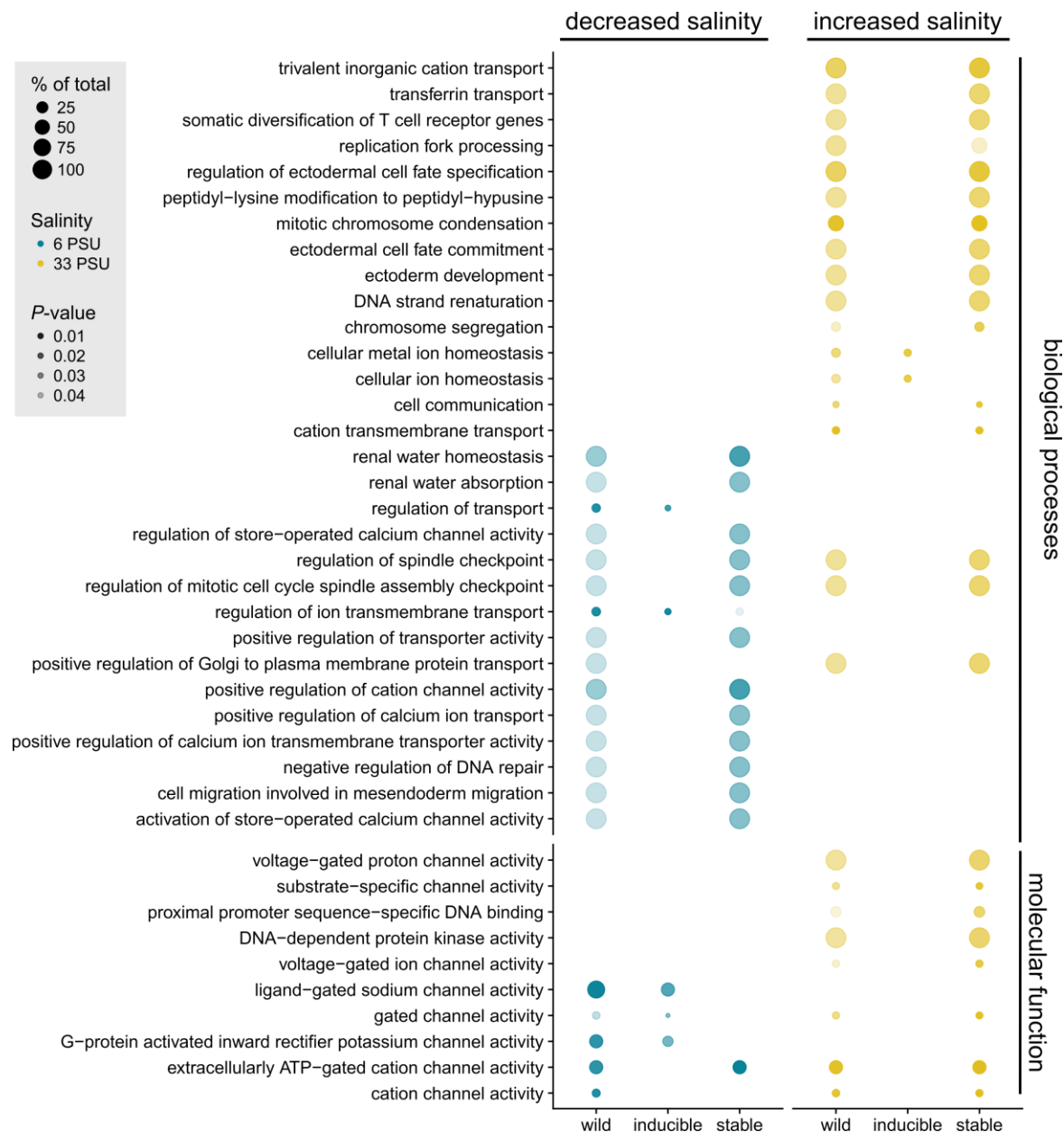
149 groups (within- and transgenerational) compared to the control group (q -value < 0.0125 ;
150 methylation difference $\geq 15\%$) this site was considered inducible. Such environment-specific
151 pop-DMS can facilitate adaptive transgenerational plasticity in response to environmental
152 changes (*sensu detection-based*⁷). After two generations of salinity acclimation, we found that
153 the majority of the pop-DMS remained stable, regardless of the direction of salinity change (926
154 pop-DMS = 63% at decreased salinity; 694 pop-DMS = 60% at increased salinity). A smaller
155 number of pop-DMS (13%) were inducible, as they showed a significant change in CpG
156 methylation upon experimental salinity decrease (198 pop-DMS) or increase (148 pop-DMS). An
157 additional 24% and 27% (346 and 316 pop-DMS respectively) differed significantly between
158 experimental treatment groups, but did not exceed the minimum threshold in differential DNA
159 methylation of 15% employed in this study. Interestingly, the number of inducible pop-DMS
160 (13%) derived from comparisons between natural populations was significantly higher compared
161 to what would be expected from a random selection of CpG sites across the genome ($< 1\%$;
162 1000 replicates; salinity decrease: $X^2_2 = 1090.7$, $P < 0.001$; salinity increase: $X^2_2 = 967.7$, $P <$
163 0.001). This shows that a proportion of the pop-DMS reflects a salinity-mediated plastic
164 response, as it is expected for *detection-based* sites⁷.

165

166 **Associating genes with stable and inducible DNA methylation**

167 We then assessed both stable and inducible pop-DMS for associations with different putative
168 gene function (Figure 2, Supplementary Figure S2). Genes associated with stable pop-DMS
169 (452 and 329 under salinity decrease and increase, respectively) were enriched for basic
170 biological processes (e.g. DNA repair, chromatid segregation), but also for osmoregulatory
171 functions (e.g. cation and proton channel activity; Figure 2). In line with mathematical models on
172 the role of epigenetic and genetic changes in adaptive evolution⁵, these stable DNA methylation
173 sites were potential targets for natural selection, resulting in differential DNA methylation
174 between locally adapted populations. Inducible pop-DMS were associated with genes (100 and

175 82 under salinity decrease and increase, respectively) that were primarily enriched for other
 176 osmoregulatory functions such as ion channel activity and homeostasis (Figure 2,
 177 Supplementary Figure S2). We take this functional association as further evidence that inducible
 178 pop-DMS, sensu *detection-based*⁷, are representing a molecular basis of adaptive phenotypic
 179 plasticity by allowing individuals to regulate their ion balance relative to the seawater medium
 180 instantaneously without requiring any further genetic adaptation at the population level.



181
 182
 183

Figure 2: Gene ontology terms for biological processes and molecular functions.

184 Gene ontology (GO) terms for biological processes and molecular functions under salinity increase
185 (yellow, 20 vs. 33 PSU) and decrease (blue, 20 vs. 6 PSU) associated with differentially methylated sites
186 between populations (pop-DMS) are presented. The graph is split into GO terms associated with pop-
187 DMS from natural stickleback populations across a salinity cline (wild) and their experimental inducibility
188 (inducible and stable) in a two-generation acclimation experiment. The size of the circles refers to the
189 number of genes of this term present in our groups (in %) and the transparency to the *P*-value (darker
190 circles refer to a lower *P*-value). This subset is filtered for GO terms including the following keywords:
191 "*anion*", "*cation*", "*channel*", "*transport*", "*water*", "*chloride*", "*potassium*", "*homeostasis*", "*DNA*",
192 "*chromatid*", "*chromosome*", "*spindle*", "*ectoderm*", "*endoderm*", see Figure S2 (Supplementary Material)
193 for the full figure.

Ensembl gene ID	chromosome	start position	end position	gene name	wild	inducible	'expected' inducible	'opposite' inducible	stable	semi-inducible	Fisher's exact (<i>P</i>)
<i>Salinity decrease:</i>											
ENSGACG00000008328	Chr10	12860144	12863850	si:dkey-166k12.1	24	0	0	0	9	15	0.005
ENSGACG00000019416	Chr7	4451892	4453656	HMX1 orthologue	17	0	0	0	9	8	0.033
ENSGACG00000013229	Chr18	15327717	15352321		15	0	0	0	3	12	0.011
ENSGACG000000017287	Chr3	13454527	13465167	mmp16b	12	0	0	0	12	0	0.001
ENSGACG000000017584	Chr3	14690814	14694448	CCNY	12	12	12	0	0	0	0.001
ENSGACG000000018249	Chr4	12141625	12143011	si:ch211-153b23.5	12	1	1	0	3	8	0.188
ENSGACG000000008034	Chr6	9368187	9380941		11	10	10	0	0	1	0.014
ENSGACG000000009469	Chr1	9166576	9173856	egln2	11	0	0	0	11	0	0.001
ENSGACG000000004433	Chr17	2127457	2211376	igsf21a	10	10	10	0	0	0	0.003
ENSGACG000000007343	Chr10	10666995	10679875	col9a2	10	0	0	0	6	4	0.227
ENSGACG000000018407	Chr4	13828336	13837518	Sncb	10	2	2	0	5	3	0.848
<i>Salinity increase:</i>											
ENSGACG000000020323	Chr7	17010160	17011176		23	0	0	0	22	1	<0.001
ENSGACG00000013229	Chr18	15327717	15352321		15	10	10	0	1	4	0.125
ENSGACG000000013359	Chr11	12960883	12968110	sec14l1	15	0	0	0	12	3	0.011
ENSGACG00000019416	Chr7	4451892	4453656	HMX1 orthologue	15	3	3	0	5	7	0.745
ENSGACG000000002948	Chr8	218240	221355	ddx10	14	0	0	0	6	8	0.077
ENSGACG000000016350	Chr14	3603545	3604923		14	1	0	1	7	6	0.277
ENSGACG000000006636	Chr18	4780893	4786820	ZC3H12D	13	0	0	0	3	10	0.034
ENSGACG000000004667	Chr12	4273498	4286193	tti1	12	0	0	0	12	0	0.001
ENSGACG000000015566	Chr2	9043062	9051779	casc4	10	0	0	0	10	0	0.003

194

195 **Table 1: Differentially methylated genes across natural populations along a salinity cline.**

196 Genes derived from DNA methylation comparisons between natural populations associated with ≥ 10 pop-DMS (decreased salinity: KIE (20 PSU) vs.
197 NYN (6 PSU); increased salinity: KIE (20 PSU) vs. SYL (33 PSU)). Ensembl gene ID and name as well as the position on the chromosome are listed.
198 The numbers refer to the numbers of DMS in the population comparison (wild). These DMS were classified into 'inducible', 'semi-inducible' and
199 'stable' sites according to their behavior in a two-generation salinity acclimation experiment with laboratory bred sticklebacks from the mid salinity
200 population (20 PSU) exposed to experimental salinity increase or decrease (33 and 6 PSU respectively). Further, inducible sites were distinguished
201 whether they matched methylation levels of the locally adapted population ('expected') or not ('opposite'). Genes written in bold vary in both population

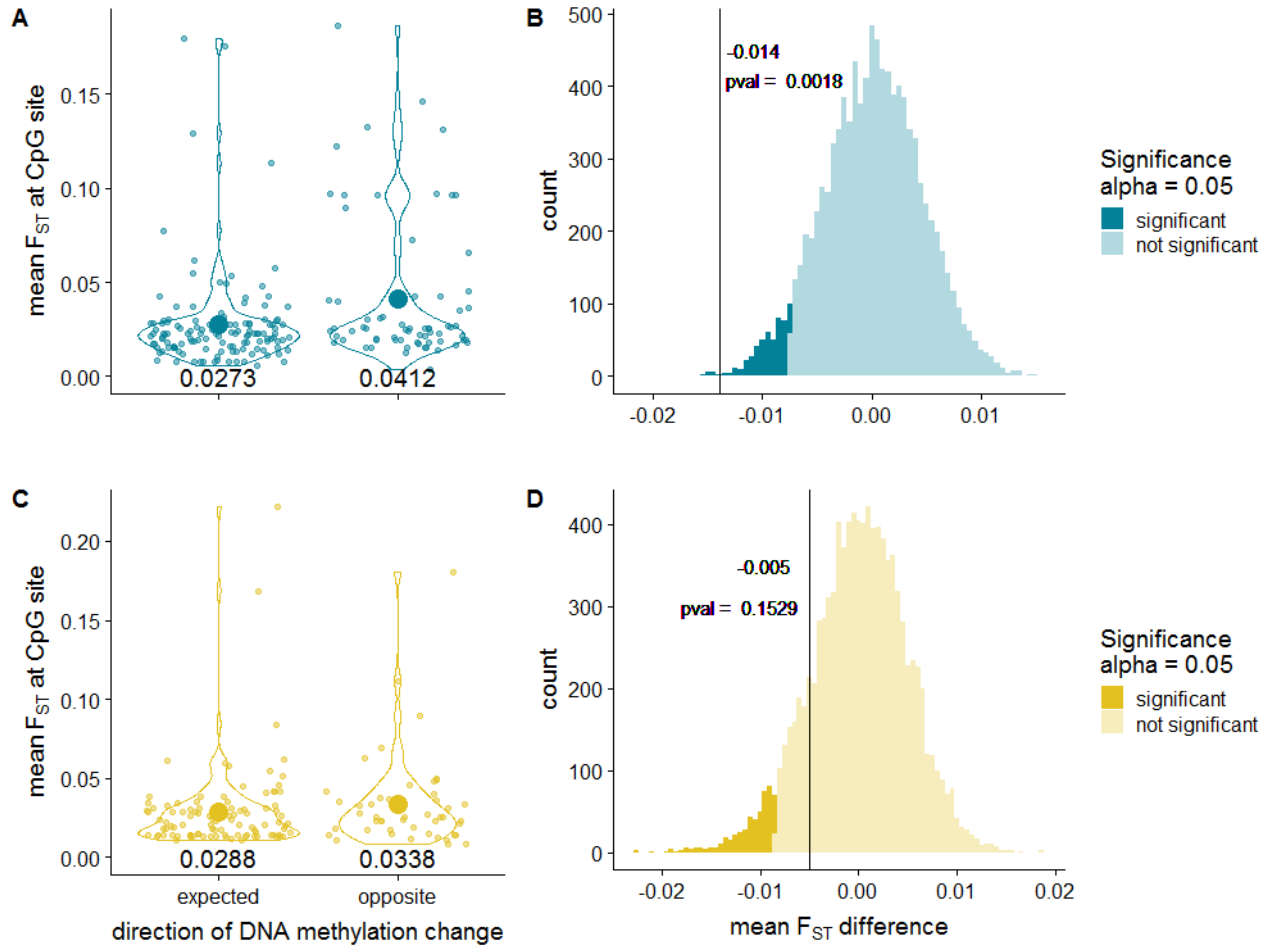
202 comparisons. We used a Fisher's exact test to assess whether pop-DMS associated to the same gene are correlated in their response to
203 experimental salinity change (non-random distribution among the categories stable, inducible, semi-inducible) and reported corresponding *P*-values.
204 For a full table on all genes associated with 1 or more pop-DMS see Table S2A and S2B (Supplementary Material).

205 **Assessing the role of experimentally inducible DNA methylation in nature**

206 We then assessed if multiple pop-DMS associated with the same gene showed a correlated
207 response to experimental salinity acclimation, which would result in a non-random distribution of
208 pop-DMS within genes among the categories ‘stable’, ‘inducible’ and ‘semi-inducible’. We found
209 that in 13 out of 20 genes with ≥ 10 pop-DMS, these pop-DMS responded similarly across the
210 gene upon salinity acclimation (Table 1, Fisher’s exact test, $P < 0.05$). This non-random pattern
211 of change provides additional evidence that we have identified inducible pop-DMS relevant to
212 the *detection-based*⁷ information pathway. Secondly, we tested whether a change at inducible
213 pop-DMS in experimental fish increased the similarity to methylation patterns found in natural
214 populations locally adapted to their respective salinity conditions. Of the 198 (decreased salinity)
215 and 148 (increased salinity) inducible pop-DMS, 130 (66%) and 101 (68%), respectively,
216 changed to become more similar to methylation levels of the locally adapted field populations
217 (hereafter ‘*expected*’ direction). Conversely, at 68 and 47 inducible pop-DMS experimental fish
218 showed methylation changes in the opposite direction, decreasing the similarity with methylation
219 levels observed in the natural populations from 6 and 33 PSU, respectively (hereafter ‘*opposite*’
220 direction). At this point, it is tempting to assume that a DNA methylation change in the *expected*
221 direction is adaptive, while a change in the *opposite* direction is maladaptive. However, since
222 correlations exist between genetic variants and DNA methylation^{31, 32}, and SNPs at CpG sites
223 may interfere with methylation function^{33, 34}, conclusive evidence requires additional genomic
224 characterization.

225 We then hypothesized that *opposite* inducible pop-DMS are associated with higher
226 genomic (DNA sequence-based) differentiation, while we anticipated the reverse at *expected*
227 inducible pop-DMS. Accordingly, we re-sequenced whole genomes of the same wild caught
228 individuals we used for RRBS and calculated the degree of genomic differentiation per inducible
229 pop-DMS as mean F_{ST} value (± 5 kb window) between populations. In line with our hypothesis,
230 the populations from Kiel and Nynäshamn (decreased salinity) were genetically more

231 differentiated at *opposite* inducible pop-DMS than at *expected* sites (δ .mean.F_{ST} = -0.014, P =
232 0.002; Figure 3A and 3B). A similar trend, yet not significant, was found between the populations
233 from Kiel and Sylt (increased salinity: δ .mean.F_{ST} = -0.005, P = 0.153; Figure 3C and 3D). Here,
234 the lack of significance may be due to increased mortality and hence selection under increased
235 salinity¹⁷. Thus, at least under decreased salinity, when experimentally induced DNA methylation
236 becomes more similar to the methylation in natural populations, this occurs in a genomic
237 background with low genetic differentiation. On the other hand, when experimentally induced
238 methylation differences to the low salinity population increase (Figure 3A and 3B), this occurs in
239 a genomic background with higher genetic differentiation. This finding underlines the importance
240 of the genomic background when interpreting DNA methylation patterns. We suggest that
241 genomic information at these regions already mirrors past selection leading to DNA-based local
242 adaptation, rendering epigenetic modifications less relevant⁵. Nevertheless, it remains to be
243 tested what happens to all induced DNA methylation sites with selection over multiple
244 generations.
245



246
247

248 **Figure 3: Differential DNA methylation between populations depends on the degree of genomic**
249 **differentiation.**

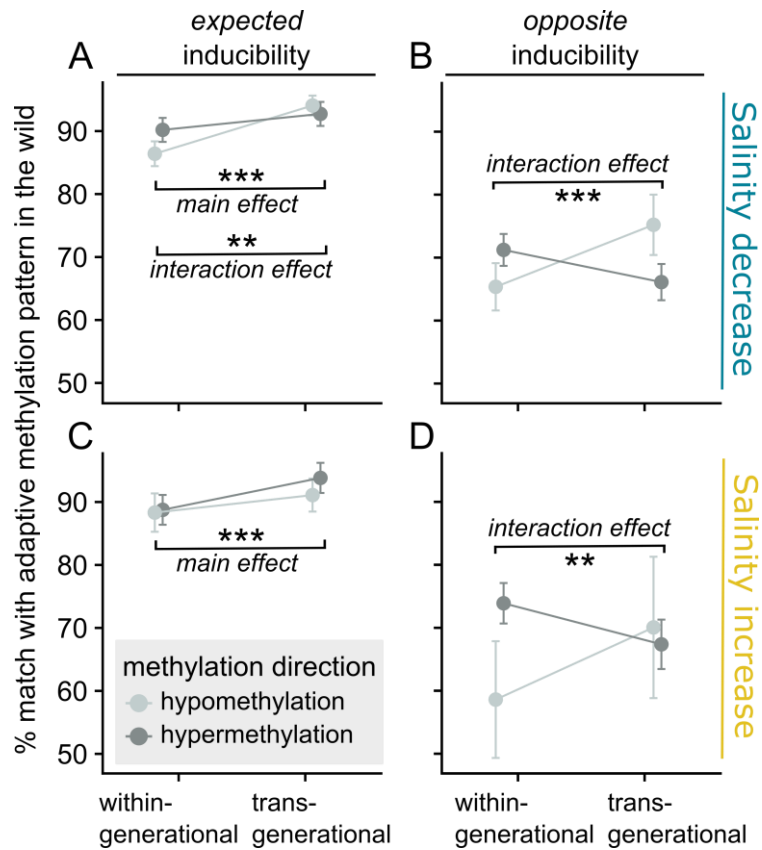
250 Figure 3A and 3C show mean F_{ST} values for pop-DMS (with a ± 5 kb window) inducible under
251 experimental salinity decrease (top, blue) and increase (bottom, yellow), that either shifted methylation
252 levels towards the values observed in the field (*expected*) or the opposite direction (*opposite*). A
253 randomization test (with 10,000 bootstraps) was performed for the difference between expected and
254 opposite mean F_{ST} value ($\delta \cdot \text{mean} \cdot F_{ST} = \text{'expected' mean } F_{ST} - \text{'opposite' mean } F_{ST}$; Figure 3B and 3D).
255 Under the one tailed hypothesis of increased genetic differentiation at *opposite* sites and an alpha of 0.05
256 the P -value was calculated as values smaller than the true difference divided by 10,000 bootstraps.

257

258 **Comparing within- and transgenerational acclimation effects on inducible DNA**
259 **methylation**

260 We then tested whether or not transgenerational plasticity of DNA methylation is adaptive. Under
261 this hypothesis, salinity acclimation over two consecutive generations compared to only within
262 generation exposure would enhance the similarity at inducible pop-DMS with patterns found
263 among wild populations at corresponding salinities. Hence, we calculated the percentage match
264 (δ .meth.diff, Figure 4) between the within- and transgenerational acclimation groups in relation
265 to the anticipated adaptive methylation level at inducible pop-DMS. We found that
266 transgenerational compared to only within generation salinity manipulation increased the
267 δ .meth.diff (for 'expected' inducible methylation: decreased salinity: $F_{1,256} = 30.42$, $P < 0.001$;
268 increased salinity: $F_{1,198} = 10.39$, $P = 0.001$; Figure 4A and C). Remarkably, we found an
269 interaction of 'methylation direction' (hyper- or hypomethylation) and 'acclimation' (within- and
270 transgenerational) affecting the δ .meth.diff under decreased salinity (ANOVA, δ .meth.diff ~
271 methylation direction * acclimation, $F_{1,256} = 7.69$, $P = 0.006$; Figure 4A). Here, transgenerational
272 acclimation increased the similarity of hypomethylated sites to methylation levels found in natural
273 populations, while hypermethylated sites showed equally similar values within- and across
274 generations (Figure 4A). While for 'expected' inducible sites this effect was only present under
275 decreased salinity, at 'opposite' inducible sites transgenerational acclimation to decreased and
276 increased salinity enhanced the δ .meth.diff at hypomethylated sites (Figure 4B and D; ANOVA,
277 δ .meth.diff ~ methylation direction * acclimation, decreased salinity: $F_{1,132} = 19.89$, $P < 0.001$;
278 increased salinity: $F_{1,90} = 9.85$, $P = 0.002$). Generally, the spontaneous addition of a methyl-
279 group to a cytosine is 2.5 times more likely than the removal³⁵ making a targeted de-methylation
280 harder to achieve. In the transgenerational acclimation group, the methylation reprogramming
281 including extensive methylation erasure and *de novo* methylation during gamete formation and
282 zygote development could serve as a mechanistic basis to enhance de-methylation of CpG
283 sites^{36, 37}.

284



285

286

287 **Figure 4: Effect of the duration of acclimation (within- vs. transgenerational) on DNA methylation**

288 **inducibility.** The y-axis shows the percentage match between the within- and transgenerational

289 acclimation group in relation to the anticipated adaptive methylation level found in natural populations at

290 inducible pop-DMS. This value was obtained by calculating the difference between the methylation

291 change in the experiment (meth.diff.exp in %; control vs. within-generational or control vs.

292 transgenerational) and the difference in methylation between natural populations (meth.diff.wild in %) as

293 $\delta.\text{meth.diff} = 100 - (\text{meth.diff.wild} - \text{meth.diff.exp})$. Mean values \pm 95% confidence interval are shown for

294 within- and transgenerational acclimation to decreased and increased salinity at *expected* and *opposite*

295 inducible sites. Colors refer to the direction of DNA methylation change (hypomethylation or

296 hypermethylation). Values closer to 100 indicate a shift in methylation pattern towards adaptive

297 methylation levels found in natural populations and stars indicate the significance level ($P \leq 0.001$ '***'; $P \leq$

298 0.01 '**') for the comparison between within- and transgenerational acclimation. 'Main effect' refers to an

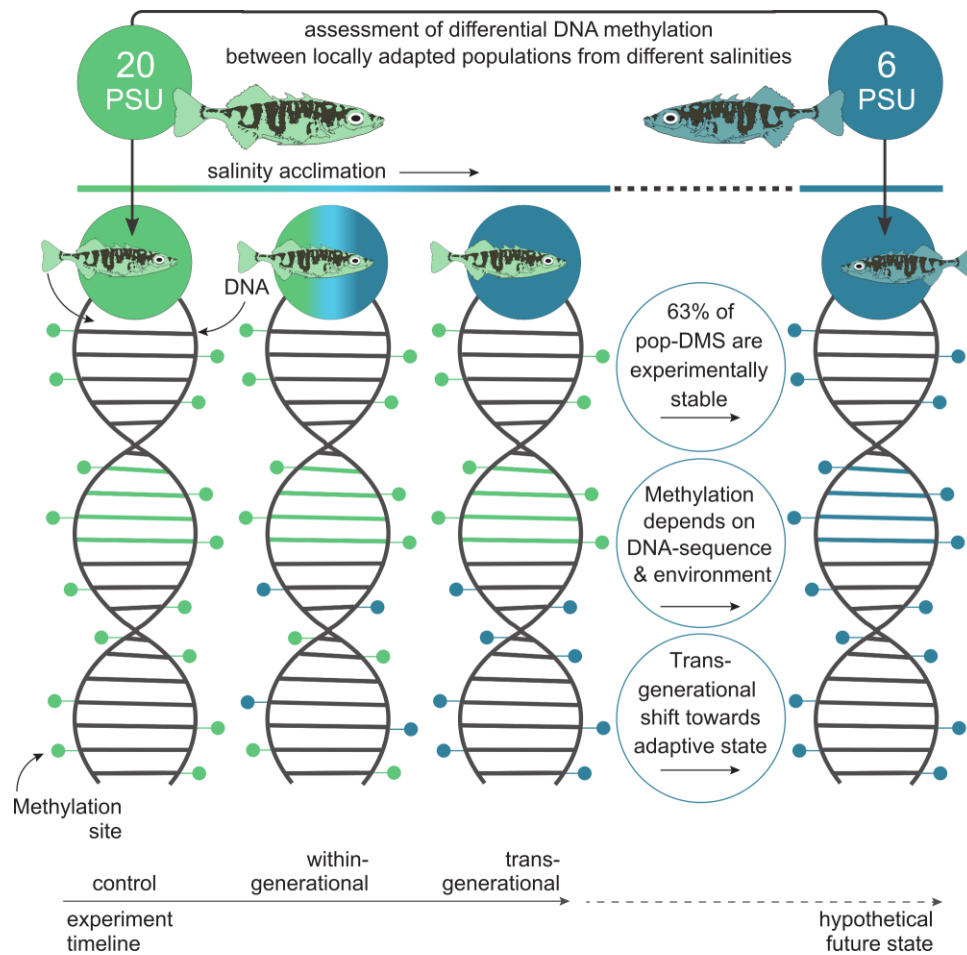
299 effect of acclimation (within- or transgenerational) and '*interaction effect*' to an interaction of acclimation
300 and methylation direction (hypo- or hypermethylation).

301

302 **Conclusion**

303 Our study provides the first empirical evidence that stable and inducible DNA methylation in
304 nature exist and follow predictions from evolutionary theory according to a *selection-* and a
305 *detection-based* epigenetic pathway to promote adaptation to novel environments^{5,7} (Figure 5).
306 Consistent with modeled selection dynamics of DNA methylation⁷, we identified DMS between
307 populations enriched for critical osmoregulatory functions insensitive to experimental salinity
308 change. Such *selection-based* (stable) methylation works along the same evolutionary trajectory
309 as adaptive DNA sequence-based evolution^{5,7}. Given expected epimutation rates of
310 approximately 10^{-4} (estimated for *A. thaliana*³⁸), the resulting phenotypic variation allows
311 populations to explore the fitness landscape faster than under DNA sequence based genetic
312 variation alone^{5,35}. On the other hand, other osmoregulatory functions corresponded to the
313 *detection-based* epigenetic pathway⁷ as they were associated with inducible DMS. This
314 inducibility accumulated in the predicted direction across generations and forms a molecular
315 basis of adaptive transgenerational plasticity. The latter has been widely discussed as potential
316 buffer of environmental changes^{10,18,39} which would allow populations to persist in the face of
317 disturbance by moving phenotypes faster in the direction of optimal fitness than genetic changes
318 alone^{5,35}. By combining experiments on the inducibility of the methylation level of certain DMS
319 with field observations on populations locally adapted to different salinity regimes¹⁵, we gained
320 unprecedented insights into the role of DNA methylation patterns in natural populations. Overall,
321 our study demonstrates that DNA methylation works alongside genetic evolution to facilitate
322 local adaptation and promote adaptive transgenerational plasticity.

323



324

325 **Figure 5: Graphical summary of experimental design and main results.**

326 We used the Baltic Sea salinity gradient to study the role of DNA methylation in local salinity adaptation
 327 and the response to salinity change in a space-for-time approach. To assess the potential future
 328 acclimatization and adaptation processes of the natural stickleback population from 20 PSU (Kiel / green)
 329 to the predicted desalination⁴⁰, we compared differences in DNA methylation at CpG sites between wild
 330 caught and laboratory bred sticklebacks. Following the experiment timeline (bottom), we compared
 331 methylation levels of the experimental control group from 20 PSU, to within- and transgenerational
 332 acclimation of 20 PSU sticklebacks to 6 PSU (DNA from left to right). The population locally adapted to 6
 333 PSU serves as the hypothetical future state in which salinities will decrease (blue, DNA on the right). The
 334 three main results are written in the circles with schematically and horizontally corresponding DNA
 335 methylation changes. (i) 63% of the DMS between the populations remained stable under experimental
 336 salinity change. (ii) The direction of experimental methylation change was dependent not only on the
 337 treatment but also on the degree of genetic differentiation between the populations (see Figure 3 for

338 results). (iii) Transgenerational salinity acclimation shifted DNA methylation patterns closer to the
339 anticipated adaptive state found in the hypothetical future population (see Figure 4 for results). For clarity,
340 only one (6 PSU) of the two foreign salinity regimes tested (6 and 33 PSU) is shown, indicated by the
341 yellow fish on the top left (see Figure 1 for full experimental design).

342

343 **Material and Methods**

344 **Animal Welfare**

345 All catches were performed under legal authorization issued by the German ‘Ministry of Energy
346 Transition, Agriculture, Environment, Nature and Digitalization’ in Schleswig-Holstein (MELUR –
347 V242-7224.121-19), by the Danish ‘Ministry of Food, Agriculture and Fisheries of Denmark’
348 (Case no: 14-7410-000227), by the Estonian ‘Ministry of the Environment’
349 (Keskkonnaministeerium - eripüügiluba nr 28/2014) and by the Swedish Sea and Water
350 Authority (Havs och Vattenmyndigheten). Ethical permission for the experiments required by
351 German law was given by the MELUR: V312-7224.121-19).

352

353 **Survey and experimental design**

354 For the field survey, we collected juvenile three-spined sticklebacks (*Gasterosteus aculeatus*;
355 31.68 ± 14.25 mm) from three different salinity regimes inside and outside the Baltic Sea (Sylt
356 (SYL), Germany (55°00'58.3"N, 8°26'22.0"E), 33 PSU, N = 16; Kiel (KIE), Germany
357 (54°26'11.8"N 10°10'20.2"E), 20 PSU, N = 16; Nynäshamn (NYN), Sweden (58°52'44.7"N
358 17°56'06.2"E), 6PSU, N = 16) in September 2014. Once collected, fish were immediately
359 euthanized using tricaine methane sulfonate solution (MS222), photographed, measured (length
360 and total weight) and stored in RNA-later (24h at 7°C, afterwards at -20°C). A cut along the
361 ventral side ensured that the RNA-later solution would diffuse into all tissues. Conserved
362 specimen were later dissected in the lab and gill tissue was separated. For the acclimation
363 experiment, we collected live adult fish from Kiel (20 PSU), which were crossed in our facilities at

364 GEOMAR to obtain ten F1 laboratory bred families, herein referred to as '*parental generation*'. At
365 nine months post-hatch we split each family into three salinity treatment groups of 10 fish each:
366 one at 33 PSU, one at 6 PSU, and one control group at 20 PSU. The salinity transition was
367 performed within 10 days by 3 PSU steps every second day. Over the entire time each group
368 was fed *ad libitum* and kept in a 20-L aquarium connected to one of three filter tanks per salinity
369 treatment. After 5 months under treatment conditions, six pure crosses per salinity treatment
370 group were performed *in vitro*, herein referred to as '*offspring generation*' (F2). Upon fertilization,
371 clutches were split and separated into different treatments (Figure 1). At three months post-
372 hatch, laboratory bred F2 sticklebacks were euthanized using MS222, photographed, dissected
373 and their gill tissue was stored in RNA-later. The age at sampling matched the estimated age of
374 the wild caught juveniles. Additionally, to the 48 wild caught individuals from Kiel, Nynäshamn
375 and Sylt that were used in above field survey, we sequenced whole genomes from gill tissue of
376 an additional three populations of sticklebacks, namely from Falsterbo, Sweden (55°24'46.6"N
377 12°55'52.3"E; 10 PSU; N = 16), Letipea (59°33'07.6"N 26°36'29.7"E; 4 PSU; N = 16) and Barsta
378 (62°51'47.1"N 18°23'51.0"E; 5 PSU; N = 16).

379

380 **DNA extraction**

381 For the field survey, DNA extraction of gill tissue (N = 16 individuals per population) was
382 performed using the DNeasy Blood & Tissue Kit (Qiagen). Further purification of the extracted
383 DNA was done with NucleoSpin® gDNA Clean-up (Macherey-Nagel). For laboratory bred F2
384 offspring of the two-generation acclimation experiment, dual extraction of whole RNA and DNA
385 was performed from gill tissue (N = 11-12 individuals per treatment group, Figure 1) stored in
386 RNAlater using the AllPrep DNA/RNA mini kit (Qiagen). Purity and quality of the extracted DNA
387 was estimated using a NanoDrop ND-1000 spectrophotometer (Thermo Fisher Scientific) and a
388 standard agarose gel (1% Agarose/TAE). DNA concentration was assessed using the Qubit®
389 2.0 Fluorometer (Thermo Fisher Scientific). To obtain a balanced sex ratio, we determined the

390 gender of the individuals using a sex-specific genetic polymorphism in isocitrate dehydrogenase
391 (IDH) with a modified protocol from Peichel *et al.* (2004)⁴¹. For the PCR (settings: once 94°C for
392 3 minutes; 30 cycles of 94°C for 30 sec, 54°C for 20 sec, 72°C for 30 sec; once 72°C for 5
393 minutes), 1 µL forward and reverse primer (5µM) was used with 4.9 µL water, 1 µL 10x buffer, 1
394 µL dNTPs (0.5 µM), and 0.1 µL DreamTaq (5 U/µL). The resulting PCR products were visualized
395 with a capillary electrophoresis on the 3100 ABI sequencer and a LIZ500 size standard. While
396 males show a heterogametic signal with two bands (at approximately 300 bp and 270 bp),
397 females lack the band at 270 bp.

398

399 **Library preparation and sequencing (Whole genome sequencing, WGS)**

400 For whole genome sequencing, the 'TruSeq Nano DNA' (Illumina) library preparation kit was
401 used according to the manufacturer's protocol by the Sequencing Facility of the IKMB, University
402 of Kiel. Ultrasonication was conducted with a 'Covaris E220' (Covaris) to shear the input DNA
403 (100 ng per sample and 350 bp insert size). Before the enrichment with a PCR step (8 cycles),
404 fragmented and bead purified DNA was ligated with adenylate at the blunt 3' ends (End repair
405 and A-tailing) and with indexing adapters. Fragments were cleaned with MagSi-NGS Prep Plus
406 Beads (Steinbrenner). Paired-end sequencing of the quality-controlled and multiplexed libraries
407 was performed on the Illumina Hiseq 4000 platform (2 x 150 bp reads).

408

409 **Quality assessment, data filtering and mapping (WGS)**

410 The command line tools of *Picard v.2.7.1* (Broad Institute 2016) were used to (i) reformat the
411 Fastq to uBAM file format and to add further values (read group etc.) to the SAM header using
412 *FastqToSam*), to (ii) mark the location of adapter sequences using *MarkIlluminaAdapters*, and to
413 (iii) reconvert the sequences to Fastq format with *SamToFastq*. The stickleback genome (here
414 Broad/gasAcu1) was indexed with *bwa index* and used as a reference for the mapping with *bwa*

415 *mem*⁴² v.07.12-r1044. To retain the meta-information from the uBAMs we used
416 *MergeBamAlignment*. *Picard* was also used to identify duplicates with *MarkDuplicates*. Basic
417 statistics were generated with *CollectWgsMetrics*, *CollectInsertSizeMetrics* and
418 *AlignmentSummaryMetrics* and summarized with *MultiQC v1.0.dev0*⁴³. A total number of
419 4,463,070,154 high-quality reads (mapping quality > Q20) was mapped resulting in a mean
420 depth of 13.84x (sd. 2.02x) and mean insert size 383.07 bp (sd. 9.40 bp, Supplementary Table
421 S3). *GATK v 3.7 HaplotypeCaller*⁴⁴ was run to determine the likelihoods of the haplotypes per
422 sample, i.e. to call SNPs and indels, which were then processed with *GenotypeGVCFs* for a joint
423 genotyping. SNPs were selected using hard filters for quality and extracted from the raw
424 genotypes with a combination of the *SelectVariants*, *VariantsToTable* and *VariantFiltration*
425 commands. *VCFtools*⁴⁵ was used in a next step, removing SNPs with a minimum quality score
426 (*minQ*) below 20 and a minor allele frequency (*maf*) greater than or equal 0.0049.

427 428 **Library preparation and sequencing (reduced representation bisulfite sequencing, RRBS)**

429 The library preparation for methylation analyses followed the Smallwood and Kelsey reduced
430 representation bisulfite sequencing (RRBS) protocol⁴⁶. A total of 100-250 ng purified DNA was
431 digested with the methylation-insensitive *MspI* restriction enzyme, which cuts at the “CCGG”
432 motif and thereby enriches for CpG regions. DNA end-repair and A-tailing was conducted and
433 un-tailed CEGX spike-in controls (Cambridge Epigenetix) were added. These are DNA oligos of
434 known sequence and with known cytosine modification, which can be used for downstream
435 assessment of bisulfite conversion efficiency. After adapter ligation, bisulfite conversion was
436 conducted using the EZ-96 DNA Methylation-Gold Kit (Zymo Research) according to the
437 manufacturer’s protocol. PCR amplification with 19 cycles were performed. Quality control of
438 purified PCR products was performed on a 2200 TapeStation System (Agilent) and high-quality
439 libraries were pooled and diversified with 15% PhiX. Single-end sequencing with 100 bp read
440 length was conducted on a HiSeq 2500 sequencer (Illumina).

441

442 **Quality assessment, data filtering and mapping (RRBS)**

443 In total 106 individuals (48 wild caught and 58 experimental fish) of balanced sex ratio were
444 DNA sequenced at an average of 19.8 ± 3.5 million reads for experimental fish and 11.4 ± 2.1
445 million reads for wild-caught fish (Supplementary Table S4). De-multiplexed fastq files were
446 quality checked using *FastQC v0.11.5*⁴⁷ and *Multiqc v1.3*⁴³. Adapters were removed with
447 *cutadapt v1.9.1*⁴⁸ using multiple adapter sequences (NNAGATCGGAAGAGCACAC,
448 AGATCGGAAGAGCACAC, ATCGGAAGAGCACAC) with a minimum overlap of one base pair
449 between adapter and read. This was necessary to remove primer dimers and avoid false
450 methylation calls systematically caused by the RRBS end-repair step during library preparation,
451 if the end repair step adds artificial cytosins. Simultaneously, *cutadapt* was used to trim low
452 quality bases ($-q 20$) from the 3'-end and remove trimmed reads shorter than 10 bases. An air
453 bubble during sequencing caused the bases 66-72 of ten tiles of one lane (affecting 12
454 individuals) to have low quality values, which were removed in a custom *awk* script. Two poor
455 quality individuals (a Sylt and a Nynäshamn female) did not meet our strict quality requirements
456 (e.g.: ≥ 5 million reads, mapping efficiency $> 52\%$) and showed biases in the proportion of
457 bases per position compared to other individuals (plot in fastqc "per base sequence content").
458 Therefore, we excluded these two libraries from downstream analysis resulting in 15 instead of
459 16 individuals from Sylt and Nynäshamn (Figure 1). Bisulfite conversion efficiency was assessed
460 from the spike-in controls (Cambridge Epigenetix), using the *cegQC software*⁴⁹. Overall
461 conversion levels were $2.4 \pm 1.8\%$ conversion of methylated cytosines and $99.6 \pm 0.5\%$
462 conversion of un-methylated cytosines, which is in line with expected conversion rates
463 (Supplementary Table S4). We used *Bismark v0.17.0*⁵⁰ to index the UCSC stickleback reference
464 genome (Broad/gasAcu1) and to generate the bisulfite alignments with *Bowtie2 v2.3.3* at default
465 settings. *Bismark* was also used to extract the methylation calls. Average mapping efficiency
466 was $63.7 \pm 2.4\%$ (Supplementary Table S4).

467

468 **Identification of differentially methylated sites**

469 The methylation calls were analyzed in *R* v3.4.¹⁵¹ using the package *methyKit* v1.3.8⁵². CpG
470 loci were filtered for a minimum coverage of 10 reads per site. To account for potential PCR
471 bias, we additionally excluded all sites in the 99.9th percentile of coverage. To improve the
472 methylation estimates, we corrected for SNPs, which could have led to a wrong methylation call.
473 The excluded positions were derived with custom written perl scripts from C-to-T and G-to-A-
474 SNPs with genotype quality of 20 and a minimum allele frequency of 0.005 (see above) from the
475 96 wild caught individuals with a combination of custom written Perl and R-scripts using
476 packages from *methykit*⁵² and *GenomicRanges*⁵³ (Supplementary File Summary_scripts.txt).
477 After normalizing coverage values between samples, using *normalizeCoverage* implemented in
478 *methyKit*, we excluded all sites that were present in fewer than 9 individuals per treatment group
479 from downstream analysis. As previously shown, sex specific methylation affects < 0.1% of CpG
480 sites on autosomal chromosomes, but > 5% of CpGs on the sex chromosome¹⁹. Therefore, to
481 exclude a potential sex bias, we removed all CpG sites located on the sex chromosomes
482 (chromosome 19), resulting in a high-quality dataset with 525,985 CpG sites. Finally, by
483 checking the first six principal components of the resulting PCA and running an ANOVA on the
484 filtered dataset, we confirmed the absence of an effect of sex on global methylation pattern
485 ($F_{124,1} = 2.611$, $P = 0.109$). However, the PCA revealed a bias in methylation pattern by families
486 over all experimental groups. Therefore, to identify differentially methylated CpG sites (DMS)
487 between treatment groups, we performed pairwise comparisons (Supplementary Table S5)
488 fitting a logistic regression model per CpG site with *calculateDiffMeth* in *methyKit* using family as
489 covariate for the experimental groups. A Chi-square test was applied to assess significance
490 levels of DMS and *P*-values were corrected to *q*-values for multiple testing using the SLIM
491 (sliding linear model) method⁵⁴. Additionally, we accounted for multiple use of groups in pairwise
492 comparisons and adjusted the alpha for the *q*-value according to Bonferroni correction to 0.0125

493 (= 0.05 / 4). Ultimately, CpG sites were considered to be differentially methylated with a q -value
494 < 0.0125 and a minimum weighted mean methylation difference of 15%. To ensure that the DMS
495 obtained are not laboratory artefacts, we used *calculateDiffMeth* implemented in *methylKit*
496 compared the wild population from Kiel to the experimental control group (Kiel population from
497 20 PSU at 20 PSU). The resulting 11,828 DMS were excluded from the DMS obtained by the
498 pairwise comparisons mentioned above (Supplementary Table S5). DMS were plotted across
499 the genome for the comparison between Kiel vs Nynäshamn (20 vs. 6 PSU, blue fish) and Kiel
500 vs Sylt (20 vs. 33 PSU, yellow fish) using *ggplot2*⁵⁵ und *hypoim*⁵⁶ (Supplementary Figure S3).

501

502 **Assessment of inducibility and gene association of DMS**

503 By comparing wild caught individuals from the mid salinity population (KIE, 20 PSU) to the
504 populations sampled at low (6 PSU, NYN) and high (33 PSU, SYL) salinity in the field, we
505 obtained 1,470 (KIE-NYN) and 1,158 (KIE-SYL) pairwise pop-DMS, which are hypothetically
506 involved in local adaptation. We first tested whether these pop-DMS distinguishing natural
507 populations are inducible or stable at the respective salinity in the experiment. A pop-DMS was
508 considered stable when the within- and the transgenerational acclimation group did not
509 significantly differ in methylation to the control group (q -value ≥ 0.0125). On the other hand, pop-
510 DMS were considered inducible when at least one of the acclimation groups was differentially
511 methylated compared to the control group (q -value < 0.0125; methylation difference $\geq 15\%$).
512 Pop-DMS with a significant q -value not exceeding the threshold of differential DNA methylation
513 (15%) will be referred to as ‘*semi-inducible*’ hereafter. We used a randomization test to ensure
514 that the number of inducible sites obtained did not occur by chance. To this end, we randomly
515 sampled 1,470 (KIE-NYN) and 1,158 (KIE-SYL) pop-DMS from the complete dataset (1,000
516 replicates). A Chi-square test was used to assess whether our observed number of inducible,
517 stable and semi-inducible sites differs from a random set of sites (averaged over replicates).
518 Finally, we tested whether the weighted mean methylation difference (meth.diff, in percentage)

519 between wild populations matches the inducible methylation difference by subtracting the
520 'meth.diff' in the experiment (exp) from the 'meth.diff' between wild caught populations (wild):

$$521 \quad \delta.\text{meth.diff} = 100 - (\text{meth.diff.wild} - \text{meth.diff.exp})$$

522 As we subtracted this difference from 100, values closer to 100 indicated higher similarity of
523 experimentally inducible methylation with the postulated adaptive DNA methylation pattern in
524 natural populations. By comparing the ' δ .meth.diff' for within- and transgenerational acclimation
525 using an ANOVA, we can assess whether there is a difference in inducibility of methylation to
526 match patterns found in wild caught populations. All analyses were run separately for decreased
527 (6 PSU; KIE-NYN) and increased (33 PSU; KIE-SYL) salinity.

528 In order to detect potential functional associations of the observed changes in DNA
529 methylation state, we classified the genomic region of a pop-DMS based on their nearest
530 transcription start site (TSS) using *annotateWithGeneParts* and *getAssociationWithTSS*
531 implemented in *genomation v1.4.2*⁵⁷. We distinguished between promoter (1500 bp upstream
532 and 500 bp downstream of TSS), exon, intron and intergenic regions. To be associated to a
533 gene, the pop-DMS had to be either inside the gene or, if intergenic, not further than 10 kb away
534 from the TSS. We excluded three pop-DMS that were on a different reference scaffold than the
535 gene they were associated to on the chrUn linkage group (that merges scaffolds into one large
536 artificial chromosome). Using the genes with associated pop-DMS, we applied a conditional
537 hypergeometric GO term enrichment analysis (P -value ≤ 0.05) with the ensembl stickleback
538 annotation dataset '*gaculeatus_gene_ensembl*' and all genes that were associated to any
539 sequenced CpG site as universe. We identified overrepresented biological processes, molecular
540 functions and cellular components using the package *GOstats v2.46*⁵⁸ in *R v3.4.1*⁵¹. Figures
541 were produced using *ggplot2*⁵⁵.

542

543 **Estimation of DNA sequence based genetic differentiation at differentially methylated sites**

544 In order to evaluate the genetic differentiation up- and downstream (in sum 10 kb) of the pop-
545 DMS position, we calculated the mean F_{ST} values ($\leq 40\%$ missing data and depth ≥ 5) from
546 whole genome sequencing data of the exact same individuals with *vcftools v.0.1.15*⁵⁹. We
547 hypothesized that inducible CpG positions matching the methylation difference *expected* from
548 the profile of the wild populations are genetically more similar between the populations than sites
549 that changed in the *opposite* direction. To test this one-tailed hypothesis we applied a
550 randomization test (with 10,000 bootstraps) on the mean F_{ST} difference between the two groups
551 (expected and opposite):

$$552 \quad \delta.\text{mean}.F_{ST} = \text{'expected' mean } F_{ST} - \text{'opposite' mean } F_{ST}$$

553 We plotted the 10,000 delta mean F_{ST} values and calculated a *P*-value by dividing the proportion
554 of values smaller than the true difference by the number of bootstraps. Figures were produced
555 using *ggplot2*⁵⁵.

556

557 **Author contributions**

558 CE and TBHR conceived and designed the study with contributions for the bisulfite sequencing
559 strategy from BSM. BSM and MJH planned and carried out the fieldwork at the German
560 locations, BSM supervised the sampling in Estonia and Sweden, which was carried out by a
561 great team of the BONUS-BAMBI project. MJH, with the help from CE and TBHR, planned and
562 supervised the breeding and acclimatization experiment. MJH and BSM conducted wet
563 laboratory work (DNA extractions and quality assessment). MPH and RH and conducted the
564 library preparation and sequencing. MJH and BSM analyzed the data and drafted the
565 manuscript together with equal contributions. All co-authors discussed and interpreted the
566 results and contributed to the final version of the manuscript.

567

568 **Data Availability**

569 Fastq raw reads of genomes and methylation sequencing will be deposited in GenBank.

570

571 **Code Availability**

572 Custom code is available as supplementary information (Summary_scripts.txt).

573

574 **Acknowledgments**

575 Many thanks to Fabian Wendt, Jakob Gismann, Linda Sartoris, Christoph Giez, Zuzanna
576 Zagrodzka, Laura Niewendick, Max Bettendorff, Bastian Poerschke, and Tobias Strickmann for
577 taking care of the experimental animals and assisting the sampling procedures. Thanks to
578 Florian R uppel for planning and constructing the recirculating aquaria systems. We thank the
579 many field helpers for catching wild sticklebacks. Many thanks also to Susanne Landis who
580 visualized our ideas in Figure 1 and 5. We kindly acknowledge the financial support for the
581 BAMBI project (Grant Agreement number: call 2012-76) by BONUS, the joint Baltic Sea
582 research program, funded by the European Union and the Federal Ministry of Education and
583 Research in Germany to TBHR and CE (reference number 03F0680A). Further, BSM's research
584 was generously supported by the Excellence Cluster 'The Future Ocean' (EXC 80) and the
585 sequencing partly by the Excellence Cluster 'Inflammation at Interfaces' (EXC 306) and 'Origins
586 and Function of Metaorganisms' (CRC1182), subprojects Z3 & INF, by the Deutsche
587 Forschungsgemeinschaft (DFG). Both 'The Future Ocean' and 'Inflammation at Interfaces' are
588 funded within the framework of the Excellence Initiative by the Deutsche
589 Forschungsgemeinschaft (DFG) on behalf of the German federal and state governments.

590

591 **Competing interests**

592 The authors declare no competing interests.

593

594 **Supplementary Information**

595 Methodological details, scripts, supplementary results, figures and tables are provided.

596

597 **References**

- 598 1. Jablonka E. The evolutionary implications of epigenetic inheritance. *Interface focus*
599 2017, **7**(5): 20160135.
600
- 601 2. Laland KN, Uller T, Feldman MW, Sterelny K, Müller GB, Moczek A, *et al.* Does
602 evolutionary theory need a rethink? *Nature News* 2014, **514**(7521): 161.
603
- 604 3. Lind MI, Spagopoulou F. Evolutionary consequences of epigenetic inheritance.
605 *Heredity* 2018, **121**: 205-209.
606
- 607 4. Bossdorf O, Richards CL, Pigliucci M. Epigenetics for ecologists. *Ecology Letters*
608 2008, **11**(2): 106-115.
609
- 610 5. Klironomos FD, Berg J, Collins S. How epigenetic mutations can affect genetic
611 evolution: model and mechanism. *Bioessays* 2013, **35**(6): 571-578.
612
- 613 6. Jones PA. Functions of DNA methylation: islands, start sites, gene bodies and
614 beyond. *Nature Reviews Genetics* 2012, **13**(7): 484.
615
- 616 7. Shea N, Pen I, Uller T. Three epigenetic information channels and their different
617 roles in evolution. *Journal of Evolutionary Biology* 2011, **24**(6): 1178-1187.
618
- 619 8. Kronholm I, Collins S. Epigenetic mutations can both help and hinder adaptive
620 evolution. *Molecular Ecology* 2016, **25**(8): 1856-1868.
621
- 622 9. Johannes F, Porcher E, Teixeira FK, Saliba-Colombani V, Simon M, Agier N, *et al.*
623 Assessing the impact of transgenerational epigenetic variation on complex traits.
624 *PLoS Genetics* 2009, **5**(6): e1000530.
625
- 626 10. Ryu T, Veilleux HD, Donelson JM, Munday PL, Ravasi T. The epigenetic landscape
627 of transgenerational acclimation to ocean warming. *Nature Climate Change* 2018,
628 **8**(6): 504-509.
629
- 630 11. Kronholm I, Bassett A, Baulcombe D, Collins S. Epigenetic and Genetic
631 Contributions to Adaptation in chlamydomonas. *Molecular Biology and Evolution*
632 2017, **34**(9): 2285-2306.
633
- 634 12. Hu J, Barrett R. Epigenetics in natural animal populations. *Journal of Evolutionary*
635 *Biology* 2017, **30**(9): 1612-1632.
636
- 637 13. Evans DH. Cell signaling and ion transport across the fish gill epithelium. *Journal*
638 *of Experimental Zoology* 2002, **293**(3): 336-347.

- 639
640 14. Reusch TBH, Dierking J, Andersson HC, Bonsdorff E, Carstensen J, Casini M, *et*
641 *al.* The Baltic Sea as a time machine for the future coastal ocean. *Science*
642 *Advances* 2018, **4**(5): eaar8195.
643
- 644 15. Guo B, DeFaveri J, Sotelo G, Nair A, Merilä J. Population genomic evidence for
645 adaptive differentiation in Baltic Sea three-spined sticklebacks. *BMC Biology* 2015,
646 **13**(1): 19.
647
- 648 16. DeFaveri J, Merilä J. Local adaptation to salinity in the three-spined stickleback?
649 *Journal of Evolutionary Biology* 2014, **27**(2): 290-302.
650
- 651 17. Heckwolf MJ, Meyer BS, Döring T, Eizaguirre C, Reusch TBH. Transgenerational
652 plasticity and selection shape the adaptive potential of sticklebacks to salinity
653 change. *Evolutionary Applications* 2018, **11**(10): 1873-1885.
654
- 655 18. Shama LNS, Mark FC, Strobel A, Lokmer A, John U, Wegner KM.
656 Transgenerational effects persist down the maternal line in marine sticklebacks:
657 gene expression matches physiology in a warming ocean. *Evolutionary*
658 *applications* 2016, **9**(9): 1096-1111.
659
- 660 19. Metzger DCH, Schulte PM. The DNA Methylation Landscape of Stickleback
661 Reveals Patterns of Sex Chromosome Evolution and Effects of Environmental
662 Salinity. *Genome Biol Evol* 2018, **10**(3): 775-785.
663
- 664 20. Artemov AV, Mugue NS, Rastorguev SM, Zhenilo S, Mazur AM, Tsygankova SV,
665 *et al.* Genome-wide DNA methylation profiling reveals epigenetic adaptation of
666 stickleback to marine and freshwater conditions. *Molecular biology and evolution*
667 2017, **34**(9): 2203-2213.
668
- 669 21. Bird A. Perceptions of epigenetics. *Nature* 2007, **447**(7143): 396.
670
- 671 22. Fraser HB. Gene expression drives local adaptation in humans. *Genome Research*
672 2013, **23**(7): 1089-1096.
673
- 674 23. Lenz TL, Eizaguirre C, Rotter B, Kalbe M, Milinski M. Exploring local immunological
675 adaptation of two stickleback ecotypes by experimental infection and
676 transcriptome-wide digital gene expression analysis. *Molecular Ecology* 2013,
677 **22**(3): 774-786.
678
- 679 24. Colosimo PF, Hosemann KE, Balabhadra S, Villarreal G, Jr., Dickson M, Grimwood
680 J, *et al.* Widespread parallel evolution in sticklebacks by repeated fixation of
681 Ectodysplasin alleles. *Science* 2005, **307**(5717): 1928-1933.
682
- 683 25. Spence R, Wootton RJ, Przybylski M, Zięba G, Macdonald K, Smith C. Calcium
684 and salinity as selective factors in plate morph evolution of the three-spined

- 685 stickleback (*Gasterosteus aculeatus*). *Journal of Evolutionary Biology* 2012,
686 **25**(10): 1965-1974.
- 687
- 688 26. Paccard A, Wasserman BA, Hanson D, Astorg L, Durston D, Kurland S, *et al.*
689 Adaptation in temporally variable environments: stickleback armor in periodically
690 breaching bar-built estuaries. *Journal of evolutionary biology* 2018, **31**(5): 735-752.
691
- 692 27. Ferchaud AL, Pedersen SH, Bekkevold D, Jian J, Niu Y, Hansen MM. A low-density
693 SNP array for analyzing differential selection in freshwater and marine populations
694 of threespine stickleback (*Gasterosteus aculeatus*). *BMC Genomics* 2014, **15**(1):
695 867.
696
- 697 28. Hohenlohe PA, Bassham S, Etter PD, Stiffler N, Johnson EA, Cresko WA.
698 Population genomics of parallel adaptation in threespine stickleback using
699 sequenced RAD tags. *PLoS Genetics* 2010, **6**(2): e1000862.
700
- 701 29. Terekhanova NV, Logacheva MD, Penin AA, Neretina TV, Barmintseva AE,
702 Bazykin GA, *et al.* Fast evolution from precast bricks: genomics of young
703 freshwater populations of threespine stickleback *Gasterosteus aculeatus*. *PLoS*
704 *Genetics* 2014, **10**(10): e1004696.
705
- 706 30. DeFaveri J, Jonsson PR, Merilä J. Heterogeneous genomic differentiation in
707 marine threespine sticklebacks: adaptation along an environmental gradient.
708 *Evolution* 2013, **67**(9): 2530-2546.
709
- 710 31. Gibbs JR, van der Brug MP, Hernandez DG, Traynor BJ, Nalls MA, Lai SL, *et al.*
711 Abundant quantitative trait loci exist for DNA methylation and gene expression in
712 human brain. *PLoS Genetics* 2010, **6**(5): e1000952.
713
- 714 32. Shoemaker R, Deng J, Wang W, Zhang K. Allele-specific methylation is prevalent
715 and is contributed by CpG-SNPs in the human genome. *Genome Research* 2010,
716 **20**: 883–889.
717
- 718 33. Gertz J, Varley KE, Reddy TE, Bowling KM, Pauli F, Parker SL, *et al.* Analysis of
719 DNA methylation in a three-generation family reveals widespread genetic influence
720 on epigenetic regulation. *PLoS Genetics* 2011, **7**(8): e1002228.
721
- 722 34. Hellman A, Chess A. Extensive sequence-influenced DNA methylation
723 polymorphism in the human genome. *Epigenetics & Chromatin* 2010, **3**(1): 11.
724
- 725 35. Van Der Graaf A, Wardenaar R, Neumann DA, Taudt A, Shaw RG, Jansen RC, *et*
726 *al.* Rate, spectrum, and evolutionary dynamics of spontaneous epimutations.
727 *Proceedings of the National Academy of Sciences* 2015, **112**(21): 6676-6681.
728
- 729 36. Potok ME, Nix DA, Parnell TJ, Cairns BR. Reprogramming the maternal zebrafish
730 genome after fertilization to match the paternal methylation pattern. *Cell* 2013,
731 **153**(4): 759-772.

- 732
733 37. Labbé C, Robles V, Herraes MP. Epigenetics in fish gametes and early embryo.
734 *Aquaculture* 2017, **472**: 93-106.
735
736 38. Schmitz RJ, Schultz MD, Lewsey MG, O'Malley RC, Urich MA, Libiger O, *et al.*
737 Transgenerational epigenetic instability is a source of novel methylation variants.
738 *Science* 2011, **334**(6054): 369-373.
739
740 39. Torda G, Donelson JM, Aranda M, Barshis DJ, Bay L, Berumen ML, *et al.* Rapid
741 adaptive responses to climate change in corals. *Nature Climate Change* 2017, **7**:
742 627–636.
743
744 40. Meier HEM. Baltic Sea climate in the late twenty-first century: a dynamical
745 downscaling approach using two global models and two emission scenarios. *Clim*
746 *Dynam* 2006, **27**(1): 39-68.
747
748 41. Peichel CL, Ross JA, Matson CK, Dickson M, Grimwood J, Schmutz J, *et al.* The
749 master sex-determination locus in threespine sticklebacks is on a nascent Y
750 chromosome. *Current biology* 2004, **14**(16): 1416-1424.
751
752 42. Li H, Durbin R. Fast and accurate short read alignment with Burrows–Wheeler
753 transform. *Bioinformatics* 2009, **25**(14): 1754-1760.
754
755 43. Ewels P, Magnusson M, Lundin S, Käller M. MultiQC: summarize analysis results
756 for multiple tools and samples in a single report. *Bioinformatics* 2016, **32**(19): 3047-
757 3048.
758
759 44. McKenna A, Hanna M, Banks E, Sivachenko A, Cibulskis K, Kernysky A, *et al.* The
760 Genome Analysis Toolkit: a MapReduce framework for analyzing next-generation
761 DNA sequencing data. *Genome Research* 2010.
762
763 45. Danecek P, Auton A, Abecasis G, Albers CA, Banks E, DePristo MA, *et al.* The
764 variant call format and VCFtools. *Bioinformatics* 2011, **27**(15): 2156-2158.
765
766 46. Smallwood SA, Kelsey G. Genome-Wide Analysis of DNA Methylation in Low Cell
767 Numbers by Reduced Representation Bisulfite Sequencing. In: Engel N (ed).
768 *Genomic Imprinting: Methods and Protocols*. Humana Press: Totowa, NJ, 2012,
769 pp 187-197.
770
771 47. Andrews S. FastQC: a quality control tool for high throughput sequence data.
772 (<http://www.bioinformatics.babraham.ac.uk/projects/fastqc>). 2010.
773
774 48. Martin M. Cutadapt removes adapter sequences from high-throughput sequencing
775 reads. *EMBnet Journal* 2011, **17**(1): 10-12.
776
777 49. CEGX Bioinformatics Team. Cambridge Epigenetix (CEGX), Babraham Research
778 Campus, Cambridge. 2015.

- 779
780 50. Krueger F, Andrews SR. Bismark: a flexible aligner and methylation caller for
781 Bisulfite-Seq applications. *Bioinformatics* 2011, **27**(11): 1571-1572.
782
783 51. R Core Team. R: A language and environment for statistical computing. *R*
784 *Foundation for Statistical Computing, Vienna, Austria* 2017.
785
786 52. Akalin A, Kormaksson M, Li S, Garrett-Bakelman FE, Figueroa ME, Melnick A, *et*
787 *al.* methylKit: a comprehensive R package for the analysis of genome-wide DNA
788 methylation profiles. *Genome Biology* 2012, **13**(10).
789
790 53. Lawrence M, Huber W, Pages H, Aboyoun P, Carlson M, Gentleman R, *et al.*
791 Software for computing and annotating genomic ranges. *PLoS computational*
792 *biology* 2013, **9**(8): e1003118.
793
794 54. Wang HQ, Tuominen LK, Tsai CJ. SLIM: a sliding linear model for estimating the
795 proportion of true null hypotheses in datasets with dependence structures.
796 *Bioinformatics* 2011, **27**(2): 225-231.
797
798 55. Wickham H. ggplot2: Elegant Graphics for Data Analysis. *Springer-Verlag New*
799 *York* 2016.
800
801 56. Hench K. <https://github.com/k-hench/hypoimg>. 2019.
802
803 57. Akalin A, Franke V, Vlahoviček K, Mason CE, Schübeler D. Genomation: a toolkit
804 to summarize, annotate and visualize genomic intervals. *Bioinformatics* 2014,
805 **31**(7): 1127-1129.
806
807 58. Falcon S, Gentleman R. Using GOstats to test gene lists for GO term association.
808 *Bioinformatics* 2006, **23**(2): 257-258.
809
810 59. Weir BS, Cockerham CC. Estimating F-statistics for the analysis of population
811 structure. *Evolution* 1984, **38**(6): 1358-1370.
812
813